Weather and Climate Extremes 33 (2021) 100327

Contents lists available at ScienceDirect

Weather and Climate Extremes

journal homepage: www.elsevier.com/locate/wace

Synoptic structure of a sub-daily extreme precipitation and flood event in Thohoyandou, north-eastern South Africa

Hector Chikoore [a,*], Mary-Jane M. Bopape [b], Thando Ndarana [c], Tshimbiluni P. Muofhe [d], Morne Gijben [b], Rendani B. Munyai [e], Tshilidzi C. Manyanya [f], Robert Maisha [b]

[a] Unit for Environmental Sciences and Management, North-West University, Vanderbijlpark, South Africa
[b] Weather Research, South African Weather Service, Centurion, South Africa
[c] Department of Geography, Geo-Informatics and Meteorology, University of Pretoria, Hatfield, South Africa
[d] Global Change Institute, University of the Witwatersrand, Johannesburg, South Africa
[e] Department of Geography, University of South Africa, Florida, South Africa
[f] Division of Nature, Forest and Landscape, KU Leuven, Leuven, Belgium

ARTICLE INFO

Keywords:
Extreme sub-daily rainfall event
Cloudburst
Floods
Tropical-temperate trough
Ridging high
Orographic lifting
Low-level jet

ABSTRACT

An extreme sub-daily precipitation event produced about 300 mm of rainfall in less than 4 h overnight from 13–14 February 2019 resulting in high floods in Thohoyandou, a small town northeast of South Africa. We employed station, radar, satellite and reanalysis datasets to investigate the rainfall, circulation and thermodynamic fields and understand the meteorological structure of the extreme event via a multiscale analysis. The large-scale synoptic environment was characterized by a mid-tropospheric tropical-temperate trough and attendant cloud band coupled to a surface high ridging over the southeast coast of the country. We found that whilst heavy rainfall (>50 mm/24 h) was widespread ahead of the upper trough, extreme amounts (~100 mm/h) were localized due to a cloudburst. A small perturbation to the favorable large scale mid-tropospheric environment also contributed to localized heavy rainfall. The south-north pressure gradient was steepened by a surface low over southern Mozambique resulting in enhanced moisture fluxes deriving from the southwest Indian Ocean. The interaction of prevailing surface winds and a low-level jet with the steep topography of the adjacent Soutpansberg Mountain Range enhanced low-level convergence and lifting in the area. We also show that the highest rainfalls were uphill of the location of flooding which was contained in a poorly drained valley. Whereas the Unified Model forecasts appeared accurate for the large-scale pattern of heavy rainfall in the area, the rainfall peak was generally underestimated, whilst the timing of extreme rainfall was delayed in the 18Z simulation, which is used by forecasters operationally. Our findings contribute to understanding the occurrence of extreme weather events over northeastern South Africa and also how models treat them, towards natural disaster risk reduction.

1. Introduction

Rainfall in South Africa exhibits strong seasonality occurring mostly during the austral summer months from October to March. The southwest of the country experiences winter rainfall whilst a narrow region on the Cape south coast receives rainfall throughout the year. In the early summer from October to December, the atmosphere over the country is largely extra-tropical and conditionally unstable (Dyson et al., 2015) but the airflow becomes more tropical and convectively unstable from about mid-December to February (D'Abreton and Lindesay 1993; Dyson et al., 2015). Precipitable water over southern Africa is largely imported from the southwest Indian Ocean (SWIO) and the Mozambique Channel (D'Abreton and Tyson 1995; Rapolaki et al., 2020) with a secondary source in the southeast Atlantic (Cook et al., 2004; Reason, 2007; Rapolaki et al., 2020) advected inland by recurved trade winds around a shallow heat low over Angola. The western tropical Indian Ocean and the south Atlantic are also important moisture sources for the region (Rapolaki et al., 2020) whilst local evaporation produces moisture for light to moderate precipitation (Trenberth 1999; Trenberth et al., 2003).

The intensity of daily rain has increased in recent years over southern Africa, most significantly during extreme rainfall days and periods (New et al., 2006; Roy and Rouault 2013; MacKellar et al., 2014; Kruger and

* Corresponding author.
E-mail address: hector.chikoore@gmail.com (H. Chikoore).

https://doi.org/10.1016/j.wace.2021.100327
Received 31 July 2020; Received in revised form 17 March 2021; Accepted 30 April 2021
Available online 12 May 2021

Nxumalo, 2017). Extreme rainfall events have become more frequent (Rapolaki et al., 2019) and are projected to persist over the sub-continent in the future climate due to an increase in concentration of anthropogenic greenhouse gases (Engelbrecht et al., 2013; Kendon et al., 2019). More importantly, sub-daily rainfall extremes are projected to become more severe than daily extremes over southern Africa by 2100, under the RCP8.5 scenario in a convection-permitting 4.5-km CP4A model (Kendon et al., 2019). Thus, despite recurrent drought seasons, heavy rainfall associated with flooding remains a distinct feature of the regional climate of southern Africa (Rapolaki and Reason 2018). Floods occur mostly during the late summer months with a peak around February (Alexander and van Heerden 1991; Rapolaki et al., 2020).

In this paper, we focus on extreme sub-daily rainfall (>200 mm/3 h) which fell in a localized area in the northeast of South Africa (Thohoyandou, Fig. 1) from 13–14 February 2019 towards the end of the 2018/19 summer rainfall season. Intense short-duration rainfall resulted in accumulation of flood waters causing damage to infrastructure and disrupting transportation and a premier league soccer match in the area. We ask what could have caused such extreme rainfall and flooding in Thohoyandou and why was it localized? Did the nearby mountain range play a role in the flood event?

Heavy rainfall events leading to flooding over northeastern South Africa are mostly related to tropical cyclone activity from the SWIO (Dyson and van Heerden 2001; Reason and Kiebel, 2004; Chikoore et al., 2015) and mid tropospheric cut-off lows (COLs, Taljaard et al., 1985; Singleton and Reason 2006, 2007b; Favre et al., 2013), but sometimes slow propagation of cloud bands (de Coning et al., 1998; Jury 2010; Hart et al. 2010, 2013; Rapolaki et al., 2019) may also result in floods. Severe thunderstorms embedded in tropical lows (Rapolaki et al., 2019) and mesoscale convective complexes (MCCs; Blamey and Reason 2009, 2012; Rapolaki et al., 2019) can also cause extreme rainfall and floods. However, MCCs tend to shift equatorward during the late summer as the atmospheric circulation becomes more tropical (Blamey and Reason 2012). A recent study by Rapolaki et al. (2019) characterized the synoptic circulation types associated with extreme daily rainfall over the Limpopo River Basin in southern Africa and found more extreme daily rainfall events over the eastern flank of the basin mostly related to cloud bands (48%).

While tropical cyclone activity over the SWIO peaks during January to February (Lindesay 1998; Singleton and Reason 2006), only about 5% of an average of nine cyclones make landfall over the east coast of southern Africa with even fewer penetrating inland (Reason and Kiebel 2004) as tropical lows. They usually re-curve southeastwards before making landfall (Reason 2007). Ex-tropical cyclones Eline in February 2000 (Reason and Kiebel, 2004) and Idai in March 2019 (Kolstad 2020) have produced the worst flooding in southern Africa claiming thousands of lives between them. Heavy rainfall and floods affecting South Africa's northeast resulting from landfall of tropical cyclones from the SWIO have been detailed in several studies (e.g. Reason and Kiebel, 2004; Reason 2007: Chikoore et al., 2015; Rapolaki and Reason 2018). This region of South Africa is most affected by tropical cyclone landfalls and associated impacts. Maisha (2014) studied extreme rainfall resulting from tropical depression Dando during the summer season of 2012 over the Limpopo region using the Weather Research and Forecasting (WRF) model and demonstrated the important role played by topography in such events.

COLs are associated with deep moist convection often resulting in persistent heavy rainfall which may cause flooding (Singleton and Reason 2007b; Ndarana and Waugh 2010) but their impact is greatest in the southern districts of South Africa, being much less frequent in the far north. However, COLs have also been found to contribute about 10% of extreme rainfall events over the northeast of South Africa (Rapolaki et al., 2019), which is the geographical focus of this study. They may occur any month of the year over the country but with a peak during the

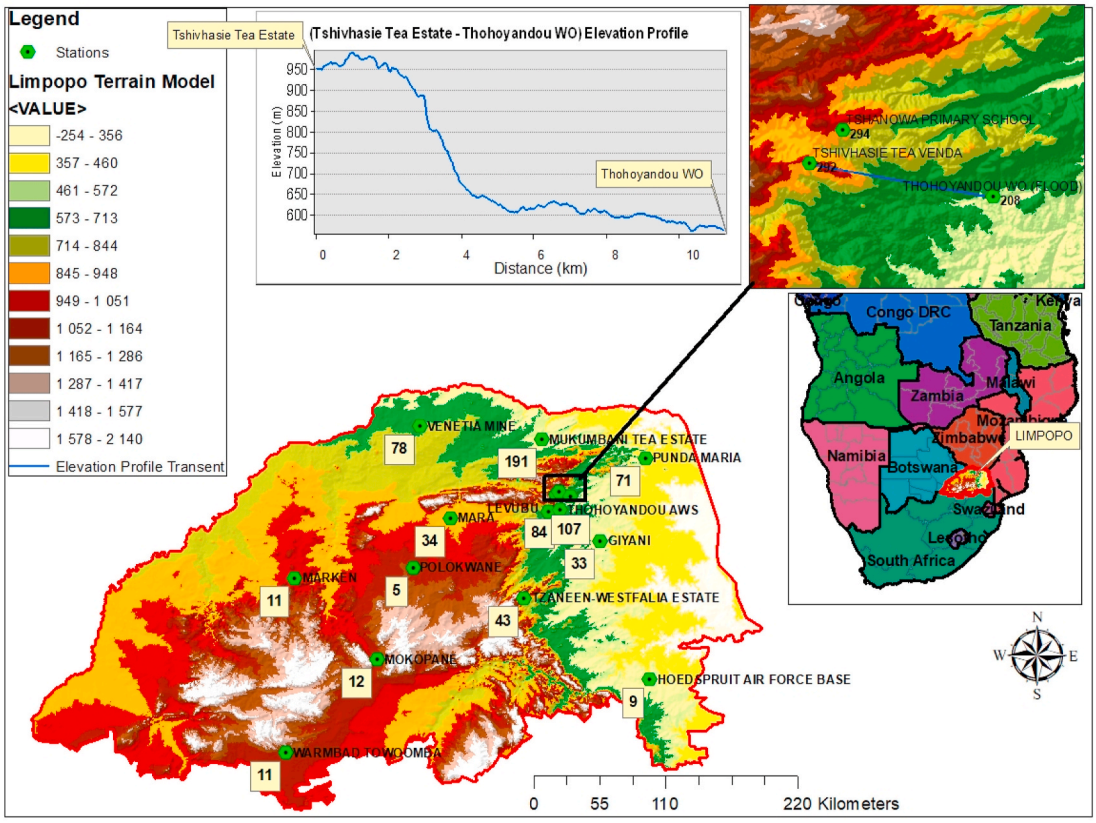

Fig. 1. The location of Thohoyandou (in black box) in Limpopo over the far northeast of South Africa. The altitude (in meters) of the flood location relative to the west-east Soutpansberg Mountain Range is also shown in an inset. The SAWS 24hr rainfall amounts (in mm) are shown in figures next to the stations.

March to May season and a secondary maximum from September to November (Singleton and Reason 2007b; Ndarana et al., 2020a).

At intraseasonal time scales, nearly half of seasonal rainfall over northeastern South Africa is produced by tropical-temperate troughs (TTTs) and attendant cloud bands (Harrison 1984; Levey and Jury 1996; Todd and Washington 1999; Fauchereau et al., 2009; Hart et al. 2010, 2013). A moist tropical low over Angola (Angola low) is linked to a westerly wave in the mid-latitudes by a TTT (Harangazo and Harrison 1983; Harrison 1984). Within this trough is a band of cloud and rain with a NW-SE orientation which links tropical convection with mid-latitude transients (Todd and Washington 1999). The frequency of tropical-temperate interactions and cloud bands over the subcontinent often determines the precipitation of a given rainfall season (Mason and Jury, 1997). Heavy and excessive rainfall may occur associated with slow eastward propagation of these troughs (Crimp et al., 1998) coupled with high amplitude westerly waves (Barclay et al., 1993). Occasionally, MCCs may also be embedded in cloud bands particularly over the northeast of South Africa (Blamey and Reason 2012).

In cases where topographic effects have a significant contribution to heavy rainfall, low-level jets (LLJs) can enhance surface forcing and hence low-level convergence and lifting (e.g. Singleton and Reason 2006; Zhao 2012; Liu et al., 2014). In a numerical simulation, an intense COL over the south coast of South Africa was impinged by the interaction of the coastal escarpment with a strong LLJ (Singleton and Reason, 2007). As a result, about 300 mm of rain fell in 24 h over East London on the south coast of South Africa in March 2002. It was also found that LLJs can result in two types of fast and slow unstable mesoscale disturbances that may resemble frontal cloud bands or squall line thunderstorms (Kuo and Seitter, 1985). Thus, there has been increased research interest in LLJs following discovery of their link to deep convective activity and enhanced transport of moisture and energy fluxes (Stensrud 1996).

Whilst several studies have detailed heavy rainfall events in South Africa (e.g. Lindesay and Jury 1991; Dyson 2009; Dyson et al., 2015; Simpson and Dyson 2018; de Coning et al., 1998; Dyson and van Heerden 2001; Rapolaki et al., 2019), most have focused on daily or multi-day timescales. Our main goal in this paper is to analyze the extreme precipitation event that occurred in Thohoyandou during February 2019 at the sub-daily timescale in order to understand the driving dynamics of this particular event and how weather models treated them. Due to the availability of high resolution datasets, we also employ a multi-scale spatial analysis approach.

The remainder of the paper is structured as follows: the study area, data and methodologies are presented next. In the results section, the evolution of the 2018/19 austral summer rainfall season and the mean state of the Pacific and Indian Oceans are discussed, for context. This is important as several studies have linked the occurrence of extreme rainfall over the subcontinent to the co-occurrence of a positive Subtropical Indian Ocean Dipole (SIOD) and the remote Pacific La Niña phenomenon (e.g. Reason and Kiebel, 2004; Reason 2007; Muller et al., 2008; Chikoore et al., 2015; Rapolaki et al., 2019). We analyze the circulation and thermodynamic anomalies including topographic influences on extreme rainfall in a small location around Thohoyandou in South Africa causing major soil erosion on the steep slopes of the Soutpansberg Mountain, sediment transport and high floods overnight from 13–14 February 2019. We also evaluate the performance of an operational numerical weather prediction model used at the South African Weather Service (SAWS), the Unified Model (UM; Davies et al., 2005) in forecasting 24-h rainfall in the area for the February 13, 2019 event. A conclusion and recommendations are offered at the end.

2. Data and methods

2.1. Study area

The main study area is located in northeastern South Africa, in the southern Limpopo River Basin and at the foot of the Soutpansberg Mountain Range with a west-east orientation (Fig. 1). Thohoyandou is a small town in a largely rural and semi-arid region of South Africa about 70 km west of the renowned Kruger National Park. Some of the highest annual rainfall amounts in South Africa (>1800 mm) are recorded west of Thohoyandou along the Soutpansberg mountain range (Levubu, Fig. 1). It is markedly drier and hotter on the rain shadow (locally called the Lowveld) north of the range. Mountains are some of the typical forcings of extreme rainfall through enhanced orographic lifting on windward slopes. Several studies have demonstrated the effect of South African topography on the circulation, providing additional forcing for extreme rainfall (e.g. de Coning et al., 1998; Crimp and Mason 1998; Singleton and Reason 2006; 2007a; Maisha 2014). The location of flooding in Thohoyandou town lies just below 600 m altitude but the adjacent Soutpansberg rises to well above 950 m over a horizontal distance of about 10 km (Fig. 1). Flooding occurred in a contained lower area of the town (Fig. 1) characterized by paved surfaces which would inhibit infiltration and drainage, promoting runoff in heavy rain. The physical location of Thohoyandou relative to the temporal propagation of winds and rainfall may help explain the role of topography in the sub-daily extreme rainfall event of 13–14 February 2019.

2.2. Observed and reanalysis data

We employ several rainfall datasets including satellite, radar and automatic weather station (AWS) data. Hourly rainfall data from SAWS was analyzed for four stations: Thohoyandou AWS, Thohoyandou WO (Weather Office), Tshivhasie Tea Estates and Tshanowa Primary School (Fig. 1) for the 24 h period from 13–14 February 2019. Reference to daily rainfall from individual weather stations is often used to define extreme rainfall events (Dyson 2009), whereas heavy rainfall is defined in this region when amounts reach and exceed 50 mm/24hr. Radar data obtained from SAWS's radar network and infrared (10.8 μm) satellite imagery from the Meteosat Second Generation satellite were used to analyze the spatial extent and propagation of convective activity and rainfall. The Rapidly Developing Thunderstorms (RDT) Tracker tool was employed to detect convective clouds and overlaid on the 10.8 μm satellite images hourly (from 14Z to 21Z) leading to the extreme rainfall event. The RDT images show different stages (growing, mature, decaying) of cloud development and the algorithm methodology has been detailed in de Coning et al. (2015). The radar quantitative precipitation estimates (QPE) are developed from the Thunderstorm Identification Tracking and Analysis (TITAN) software, converting reflectivity measurements of cloud droplets (in decibels) to rainfall rates in mm/h every 6-min using the Marshall Palmer Z-R relationship (Marshall and Palmer 1948). The 6-min rainfall rates are accumulated to obtain the amount of rainfall per hour in mm. The radar imagery displayed here is a composite of all the SAWS radars, but zoomed into the northern parts of South Africa where hourly accumulations from 16 to 22Z on February 13, 2019 are shown.

To establish the large scale rainfall distribution, the Climate Hazards Infrared Precipitation with Stations (CHIRPS; Funk et al., 2015) rainfall data were obtained and mapped via the Google Earth Engine portal (https://developers.google.com/earth-engine/). The CHIRPS data are merged from rain gauges, satellite infrared estimates and developed especially for regions of complex topography (Funk et al., 2015) such as the study area (Rapolaki et al., 2019). The high spatial resolution ($0.05^\circ \times 0.05^\circ$) CHIRPS data were employed here to map the spatial extent of heavy rainfall over southern Africa during 13–14 February 2019 and also the seasonal rainfall anomaly (October 2018–April 2019) over the subcontinent. Rapolaki et al. (2019) also used CHIRPS gridded data to analyze daily extreme rainfall events over the Limpopo River Basin, a catchment in which Thohoyandou is located.

We analyze daily and hourly mean maps of high resolution (~31 km) ECMWF ERA5 reanalyses (Hersbach et al., 2020) circulation variables which include surface pressure, horizontal winds at 850 hPa, whilst

geopotential heights and vertical velocity (omega) are analyzed in the mid-troposphere (500 hPa). Large-scale velocity potential is analyzed in the upper air at σ = 0.2101 using the NCEP/NCAR Reanalysis 2 available at 2.5 × 2.5° resolution (Kalnay et al., 1996). Sigma (σ) levels are vertical coordinate systems based on $\sigma = P/P_s$ where P is pressure level and P_s is surface pressure. Upper level (σ = 0.2101) velocity potential is closely associated with the divergent component of the horizontal wind sometimes called the irrotational wind. It is a proxy for the divergence field where negative/positive values imply upper divergence/-convergence which usually indicate low-level convergence/divergence and uplift/subsidence in intermediate levels (D'Abreton and Tyson 1995). The temporal evolution of the surface (10 m) wind (direction and strength) is also presented with 5 min wind gusts from SAWS AWS data. Whilst mean daily maps of the wind vector are important to show the large-scale controls of the circulation, they do not indicate the occurrence of gusts of strong or gale force winds.

Due to differences in elevation between the east coast (Mozambique) and the rest of the interior plateau, a shallow surface low over Mozambique is not identifiable if we analyze the 850 hPa constant pressure surface only, hence the need for analysis of MSLP. Several other studies have used hand-analyzed MSLP synoptic charts over southern Africa obtained from SAWS (e.g. Dyson and van Heerden 2001; Dyson and van Heerden 2002; Reason and Kiebel, 2004; Rapolaki and Reason 2018). The NCEP Optical Interpolated (OI) sea-surface temperature (SST) v2 data available at ¼° resolution (Reynolds 1993) were used to analyze the early summer SST anomalies in the Indian and Pacific Oceans. The OI SST v2 combine satellite observations with ships and buoy data which are interpolated on a regular grid (Reynolds 1993). We employ multiscale analysis, beginning with the synoptic scale to show the dominant controls, then focus on a smaller sub-domain covering the Limpopo River basin to identify mesoscale and local perturbations.

Over much of sub-Saharan Africa, upper air soundings are largely absent due to the high costs of tracking equipment and disposable radiosondes usually procured from European suppliers. However, in South Africa there are a few operational upper air stations that launch and track upper air ascents twice every day at midnight and midday. Here, we use SAWS tephigrams to show the vertical upper air profile (850-100 hPa) for Pretoria (Irene) station launched on 13 and February 14, 2019 at 12Z and 00Z, obtained from the University of Wyoming, Department of Atmospheric Science via their web portal (http://weather.uwyo.edu). A tephigram (similar to a skew-T/log-P diagram) is an aerological diagram that provides important diagnostics about the thermodynamics of environmental air and the vertical stability and wind profile in an area. The Pretoria profile is considered here as a proximity sounding for Thohoyandou and will help characterize the large scale environment and vertical wind (shear) structure associated with the extreme rainfall. Rasmussen and DO Blanchard (1998) considered a sounding made within 400 km of an event to be a proximity sounding in their study of supercell storms and tornadoes in the United States.

2.3. Unified Model forecasts

The UK Met Office's UM (Davies et al., 2005) is run operationally by SAWS to produce daily weather forecasts including rainfall at a horizontal grid length of 4.4 km. The simulations are made for up to 72 h lead time, and output is written with a 1-h time step. The UM was developed as a seamless model suitable for high-resolution short-range weather forecasts through to the coarser multi-decadal climate simulations (Brown et al., 2012). The model is run over the Southern African Development Community (SADC) domain and provides simulations of precipitation and other dynamic and thermodynamic variables for use as guidance in public and aviation weather forecasts and to develop products for other weather sensitive sectors. Here we present UM forecasts for the extreme rainfall event in Thohoyandou and evaluate their performance against observations. We analyze the rainfall and circulation variables for the 18Z run produced the day preceding the event which is used by forecasters to generate public weather forecasts and other specialized products. We evaluate the performance of the UM for this heavy rainfall event in terms of (1) timing of peak rainfall and (2) establish the spatial distribution of the rainfall using the eyeball verification technique (Gordon and Shaykewich, 2000). While it is important to forecast accurately the amounts associated with an extreme rainfall event, precise timing of the event is critical. Hit (good) forecasts lead to effective early warnings and disaster risk reduction, saving lives, livelihoods and property.

3. Results and discussion

3.1. Frequency of extreme rainfall in the study area

As indicated in the introduction, the study area experiences extreme rainfall events mainly from either tropical cyclones, cut-off lows, slow moving cloud bands or mesoscale convective systems. The area is also prone to droughts which are mostly linked to El Niño events or a positive Indian Ocean Dipole. Here we show the occurrence of extreme daily rainfall using CHIRPS data from 1979 to 2020 (Fig. 2). It is shown that extreme rainfall amounts exceeding 100 mm/24 h are very rare in Thohoyandou. The most extreme rainfall event in the 40 year time series occurred in February 2017, and may be related to the landfall of tropical cyclone Dineo. Other prominent peaks such as in 1996, 2000 and 2012 are also linked to cyclones Bonita, Eline and Dando which also affected the northeast of South Africa. It has been shown that the highest frequency of extreme daily rain over the Limpopo River Basin occurs in the late summer from January to March (Rapolaki et al., 2020). It is also shown here in Fig. 2b that daily rain exceeding 100 mm occurs in the late summer on the 97th percentile.

3.2. Seasonal climate anomalies

The 2018/19 summer rainfall season was largely drier than normal over much of southern Africa (Fig. 3) in a season punctuated by several extreme rainfall events over the east and southeast. Some of the positive rainfall anomalies over northern Mozambique were associated with landfall (near the coastal city of Beira) of an intense tropical cyclone (Idai) during March 2019 (Kolstad 2020). Before the country recovered from its impacts, cyclone Kenneth made landfall and flooded the far northern region of Mozambique later in April 2019 (Mawren et al., 2020). Cyclone Kenneth became the most intense tropical cyclone to make landfall on the Mozambique coastline, and its track was anomalously farther north than previously (Mawren et al., 2020). In a previous drought season in 2012, tropical depression Dando also brought extreme rainfall and flooded parts of northeast South Africa including the Kruger National Park (Maisha, 2014; Chikoore et al., 2015). Positive anomalies over South Africa's Durban (east) coast (Fig. 3) may be related to a severe COL that dumped nearly 200 mm and claimed 85 lives in late April 2019 and the event was detailed by Muofhe et al. (2020).

Whilst the relationship between the oceans and the atmosphere over southern Africa is complex (Blamey et al., 2018), the early summer was characterized by a positive Indian Ocean Dipole (IOD; Saji et al., 1999) mode with warmer SSTs in the western tropical Indian Ocean and a cooler east (Fig. 4). A positive IOD has been linked to dry conditions/drought in southern Africa but floods in East Africa (Manatsa and Matarira 2009) particularly during the early summer. The IOD also affects the seasonal climate of Australia and the Indonesian region. Cooler SSTs (by about 1 °C) prevailed in the SWIO (Agulhas; Fig. 4), suggesting negative SIOD conditions, and this region of the subtropical Indian Ocean is a major source of moisture for heavy rainfall events over the Limpopo River Basin (Crimp and Mason 1998; Rapolaki et al., 2020). Cooler conditions there would suggest reduced moisture fluxes from that source region. SST anomalies in the eastern equatorial Pacific were positive and the season was classified as a weak El Niño event (Fig. 4). Most droughts in southern Africa have occurred in the presence of El

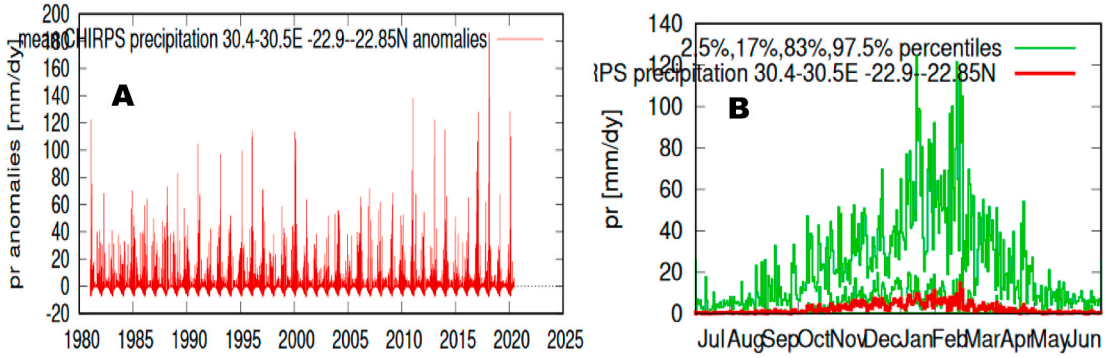

Fig. 2. (a) Anomalies of area-averaged daily CHIRPS rainfall data in the study area and (b) Mean annual cycle of rainfall (in red) and percentiles in green. . (For interpretation of the references to colour in this figure legend, the reader is referred to the Web version of this article.)

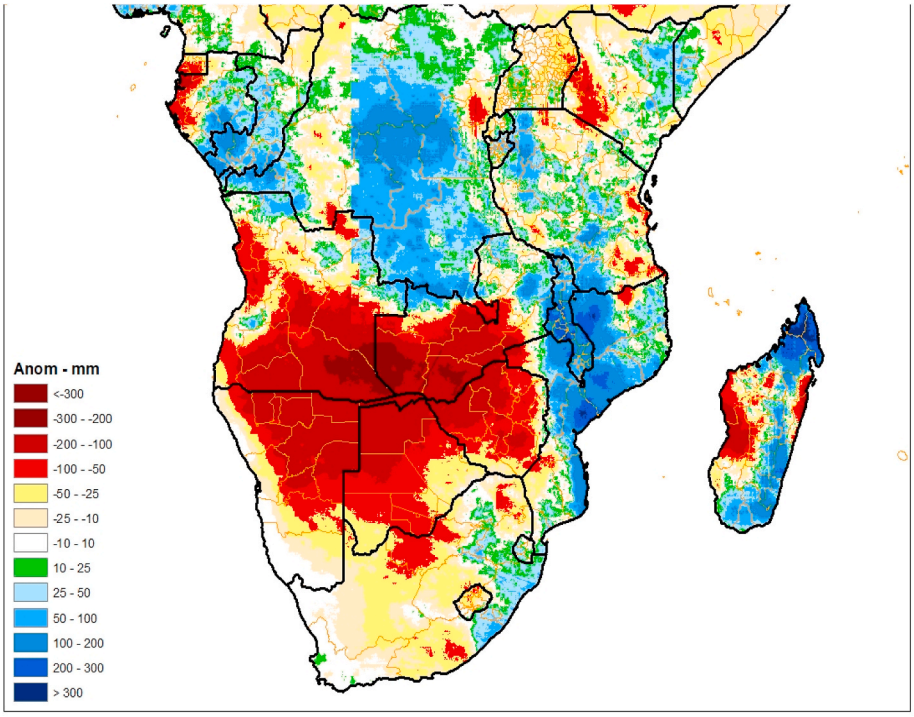

Fig. 3. Composite mean monthly anomaly (based on a 1981–2010 climatology) of CHIRPS precipitation (in mm) over southern Africa during the austral summer season from October 2018 to April 2019.

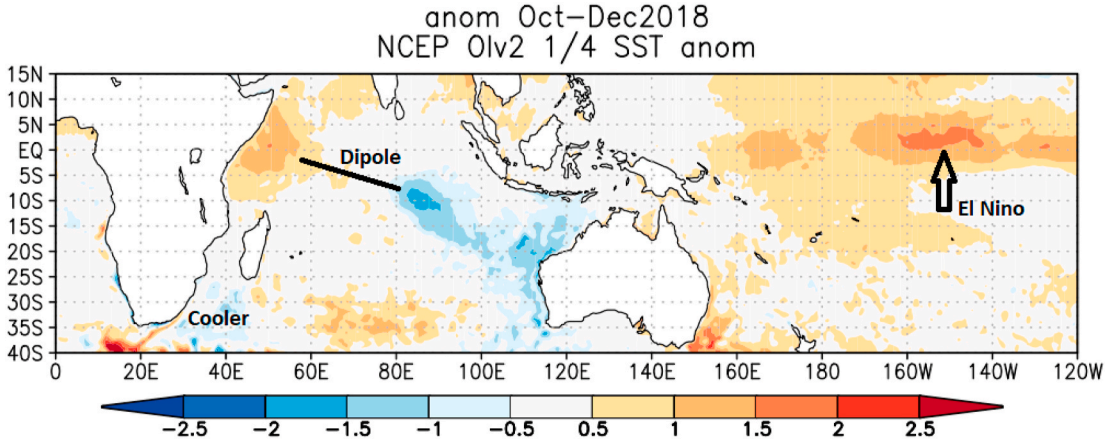

Fig. 4. Indian Ocean and Pacific SST anomalies (based on a 1981–2010 climatology) for the period Oct–Dec 2018 (in °C). The Indian dipole, cooler conditions in the SWIO and Pacific El Nino signals are highlighted.

Niño (Ratnam et al., 2014). TTTs, convective activity and cloud bands tend to relocate to the warm Indian Ocean east of Madagascar during drier summers over southern Africa (Chikoore and Jury 2010; Hart et al., 2018). When a positive IOD and El Niño co-occur, a major drought is highly probable in the region (Manatsa and Matarira 2009) such that heavy rainfall events are less likely. Rapolaki et al. (2019) found that extreme rainfall events tend to be more common during La Niña events over southern Africa than during an El Niño. Tropical cyclone activity and landfalls are rare over the Mozambique coast during El Niño, yet the SWIO experienced the highest number of tropical storms and intense tropical cyclones during this season (Mawren et al., 2020). The landfall of two most intense cyclones Idai and Kenneth over Mozambique a few weeks apart was therefore highly anomalous.

3.3. Observations of cloud and precipitation

For the 13–14 February extreme event, widespread rainfall affected the southeast of Africa extending from the equatorial Congo region through Zambia toward southern Mozambique (Fig. 5a). Heavy rainfall (>50 mm/24 h) occurred mainly in the Limpopo River Basin bordering Zimbabwe and South Africa but was more widespread over southern Mozambique (Fig. 5a and b). Floods also occurred in southern Mozambique in a country perennially susceptible due to its low altitude and vulnerability to tropical storms. It is shown here that most of the 24 h rainfall amounts fell in 3 h over Thohoyandou (Figs. 6–8), an indication of the high rainfall intensity and its associated impacts.

The heavy falls of rain were focused over the extreme north of South Africa extending from Punda Maria (71 mm) to Venetia Mine (78 mm, Fig. 1). The spatial patterns show a clear local maximum in the Thohoyandou area with a marked decrease southwards. The impact of enhanced lifting in the northeastern escarpment is also shown typically on the rainfall of Tzaneen Westfalia Estate (43 mm). The extreme rainfall of 13–14 February 2019 at Thohoyandou was preceded by a 6 day dry spell but marked the start of a wet spell with subsequent falls of 13.6 mm (14th), 18.0 mm (15th) and 3.4 mm (16th) recorded according to SAWS AWS data (not shown).

RDT satellite imagery shows the presence of a large mature cloud system southeast of Thohoyandou at 16Z (Figs. 6a) and 17Z (Fig. 6b). At 18Z (Fig. 6c) the cloud system started growing but has propagated further east from Thohoyandou with another mature cell visible over the southern part of Zimbabwe. At 19Z (Fig. 6d) several small cloud cells are visible over the Thohoyandou area which were responsible for the heavy rainfall. At 20Z (Figs. 6e) and 21Z (Fig. 6f) the large cloud system that was seen over Zimbabwe moved towards the south but produced mostly stratiform rainfall over Thohoyandou consistent with the radar QPE observations in Fig. 7.

The hourly QPE accumulations from radar also show localized heavy rain. Between 16Z and 17Z light rain was observed south of Thohoyandou (Fig. 7a) from where the cloud cell moved over the area between 17Z and 18Z (Fig. 7b) producing between 20 and 25 mm of rainfall in the core of the cell. Hourly accumulations between 18Z and 19Z (Fig. 7c) as well as between 19Z and 20Z (Fig. 7d) show rainfall totals of between 50 and 60 mm. As the storm propagated over Thohoyandou, 10–13 mm of rainfall was recorded between 20Z and 21Z (Fig. 7e) and less than 10 mm between 21Z and 22Z (Fig. 7f). It should be noted that while QPE from radar are an excellent alternative to rain gauge measurements with high spatial and temporal resolution, several limitations do exist. Errors may be present in the radar reflectivity measurements, the conversion from reflectivity to rainfall estimates, as well as the hourly accumulations of the 6-min interval rainfall estimates. The sampling of reflectivity may be influenced by several factors, including ground clutter, the bright band, attenuation, beam blockages, hail, as well as biases due to increases in observation volume with distance from the radar (Chumchean et al., 2006). In the conversion from reflectivity to rainfall estimates a single Z-R relationship like the Marshall and Palmer relationship does not take into account variations in storm type such as convective and stratiform variations in precipitation processes, as well as other effects such as measuring the ice phase above the melting layer rather than the rain below, orographic effects, and evaporation between the cloud and the ground to name a few (Steiner et al., 1999). The hourly accumulations of the individual 6-min fields may also produce errors related to the time interval between scans. A full three-dimensional radar scan takes 6-min to complete the 360-degree scans at multiple elevations, and as such each portion of the storm is sampled with a 6-min temporal resolution. This may result in a wavy pattern of concentric circles in hourly accumulations and may also affect the rainfall intensities as well as spatial and temporal distribution. With these caveats in mind, it is reasonable to expect some differences in rainfall estimates from radar when compared to rain gauge observations.

According to data from SAWS automatic rain gauges, the rain started between 20.00 h and 21.00 h local time (between 18Z and 19Z) in the Thohoyandou area, dumping about 300 mm in 3 h (Fig. 8a). Extreme rainfall resulted in flooding and damage to vehicles which were parked at a local shopping mall and football stadium.

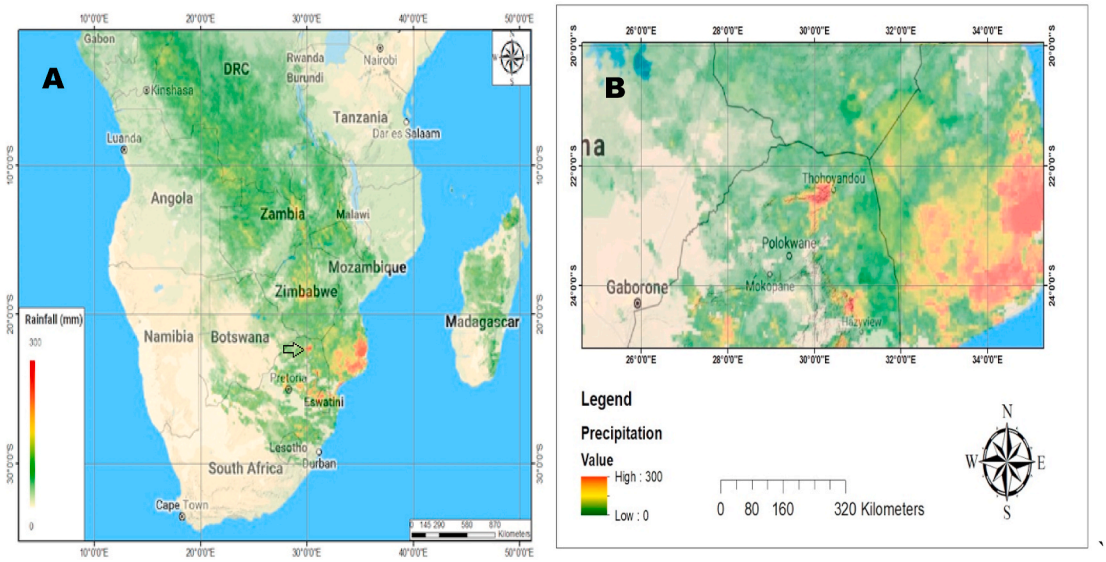

Fig. 5. (a) CHIRPS satellite-derived 24-h precipitation estimates (in mm) over southern Africa for Feb 13, 2019. A more detailed distribution of rainfall in the Limpopo River valley and southern Mozambique is shown in (b).

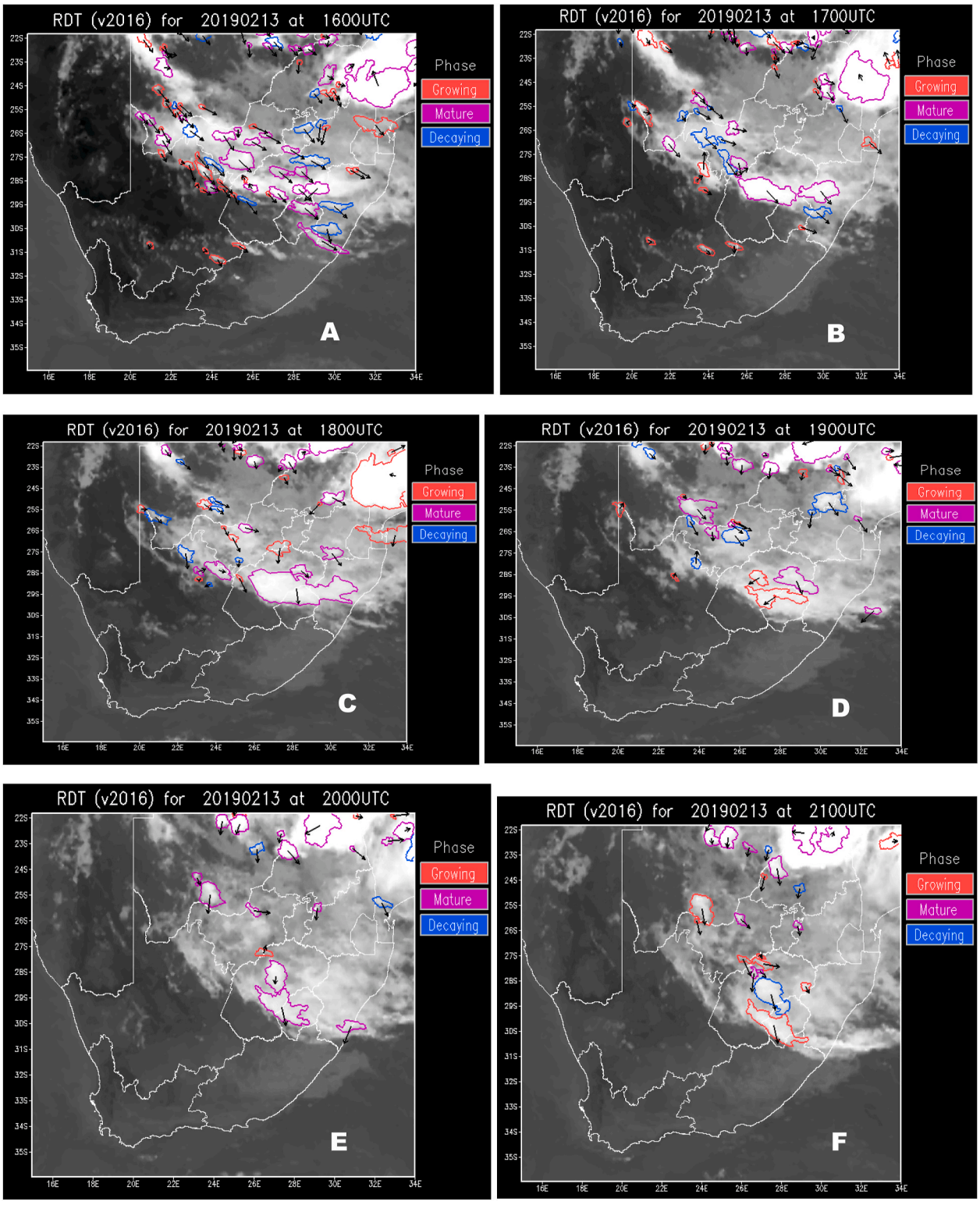

Fig. 6. RDT satellite images showing the development and propagation of the cloud systems that produced extreme rainfall over the northeast of South Africa at (a) 16Z (b) 17Z (c) 18Z (d) 19Z (e) 20Z and (f) 21Z on February 13, 2019.

In this study, 24 h rainfall amounts recorded by stations in the Thohoyandou area are shown in Table 1 and Fig. 1 with hourly data in Fig. 8a. It is shown that the highest station rainfall amounts were measured at Tshanowa Primary School (294 mm) and Tshivhasie Tea Estate (272 mm) which lie uphill of the flooding location in Thohoyandou. The flooding occurred a few feet from the Thohoyandou WO which recorded 208 mm of rainfall in a few hours, compounded by high runoff from uphill. Fig. 8a shows that the peak rainfall in the lower elevation stations (where the flooding occurred) at Thohoyandou WO and Thohoyandou AWS occurred an hour earlier than the peak uphill at Tshivhasie and Tshanowa. Thohoyandou WO recorded 97.2 mm in 1 h between 18 and 19Z whilst Tshanowa received 95.8 mm between 19 and 20Z on February 13, 2019. Such often localized extreme amounts of ~100 mm/h leading to floods have been related to the occurrence of a

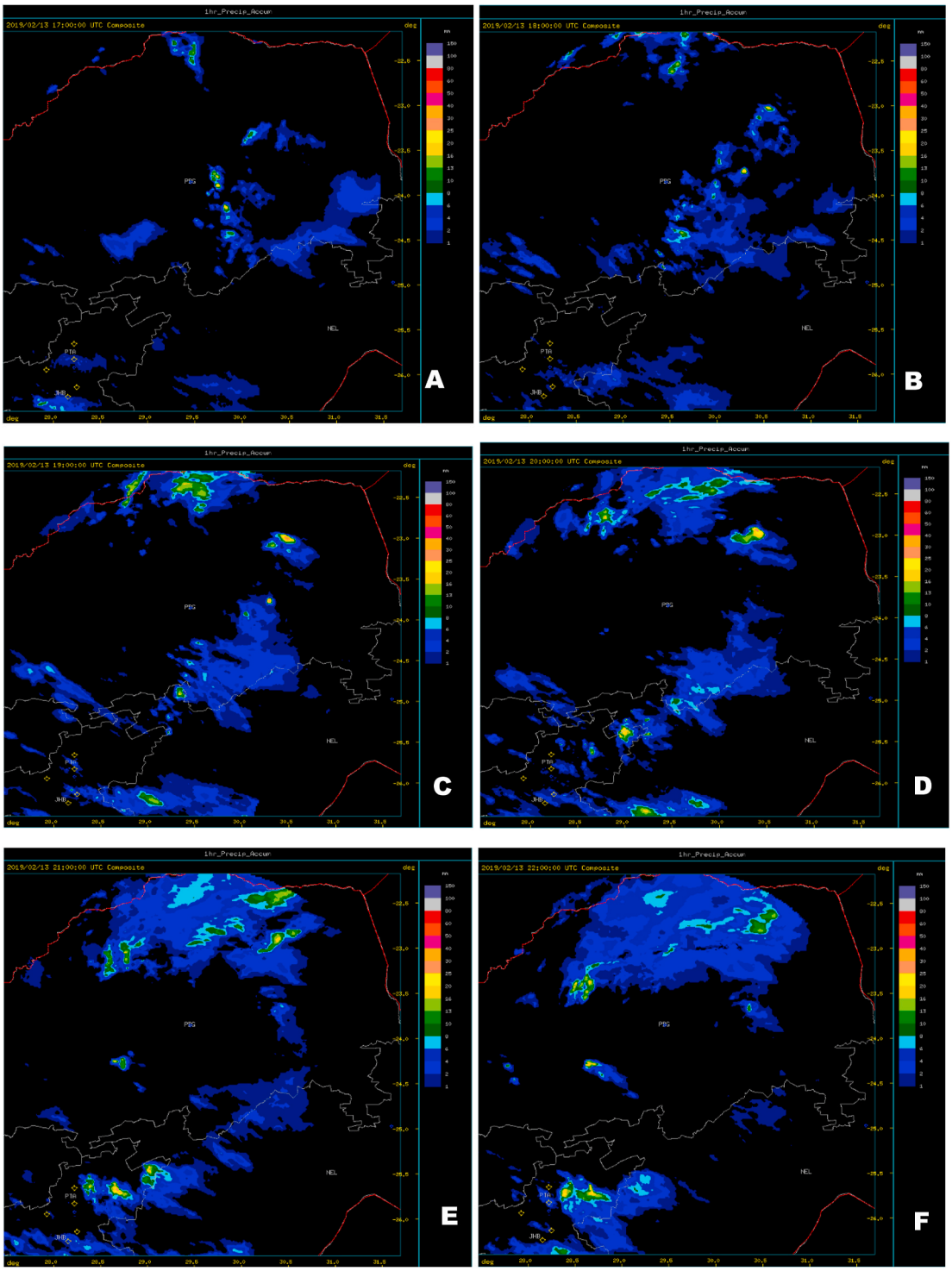

Fig. 7. Radar QPE accumulations of precipitation over the northeast of South Africa during February 13, 2019, hourly from (a) 16-17Z (b) 17–18 Z (c) 18-19Z (d) 19-20Z (e) 20-21Z and (f) 2Z-22Z.

cloudburst. This also suggests that the direction of propagation of the band of heavy rain was from east to west which could be a proxy for low level winds such that the heaviest rain was downwind (in agreement with Fig. 6). It is reasonable to deduce that, considering the elevation, the heavier rainfall uphill would have produced high runoff toward Thohoyandou WO accumulating as flood waters there (Fig. 1, inset).

Comparable extreme daily rainfall amounts (300 mm/24 h) have been recorded in South Africa during December 2006 over the central interior (Viljoensdrift) associated with a deep low at the surface drawing moist air from Botswana and Zambia (Dyson 2009). Remarkably, heavy rainfall and floods also occurred over the study region (northeast of South Africa) at about the same time during 12–14 February 1996 (de Coning et al., 1998; Crimp and Mason 1998). Several stations reported 24 h rainfall totals exceeding 100 mm during that time, and the highest falls were recorded at Zwartrandjes with 275 mm and a 3-day total of 374 mm (de Coning et al., 1998).

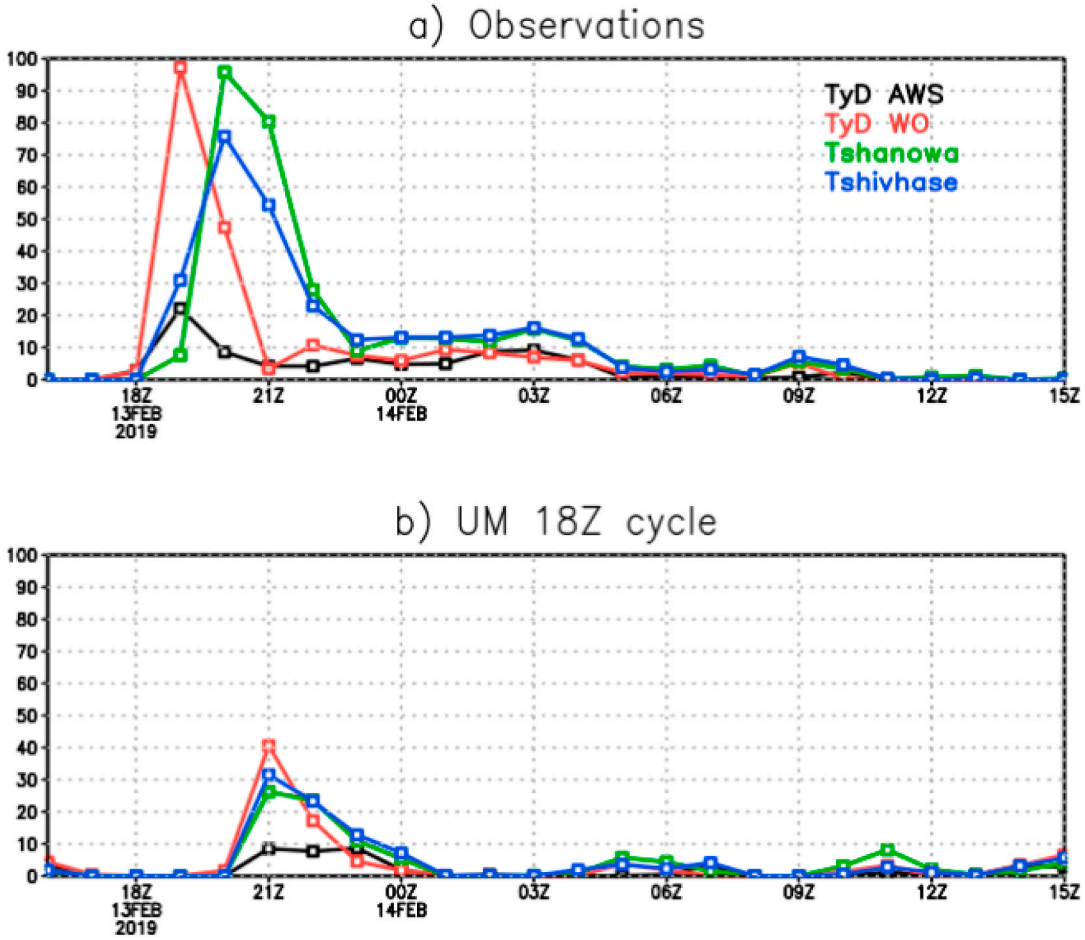

Fig. 8. (a) Hourly observations of rainfall amounts from SAWS automatic weather stations at Thohoyandou (Tyd AWS), Thohoyandou Weather Office (Tyd WO), Tshanowa Primary School (Tshanowa) and Tshivhasie Tea Estates (Tshivhase) from 13–14 February 2019. The UM rainfall simulations are shown in (b) from the 18Z cycle.

Table 1
SAWS 24-hr rainfall totals for February 13, 2019 in the Thohoyandou area.

Station Name	Rainfall amounts (mm)
Mukumbani Tea Estates	191
Thohoyandou AWS	84
Thohoyandou WO	208
Tshanowa Primary School	294
Tshivhasie Tea Estates	272

3.4. Synoptic situation

Synoptic events preceding the flood event from 13–14 February 2019 in Thohoyandou were characterized by the development of a TTT and attendant cloud band from about February 11, 2019 (Fig. 9). The cloud band remained quasi-stationary over the subcontinent but it only started raining over Thohoyandou on the 13th, lasting several days according to SAWS data. Slow propagation of TTTs can lead to heavy/extreme rainfall in an area in southern Africa (Hart et al., 2010). By February 13, 2019, the synoptic scale mid-tropospheric (~500 hPa) circulation was characterized by a westerly wave and a rotating low embedded over northern Botswana, coupled with an advecting high over the Mozambique Channel which were steering warmer tropical air toward the study area (Fig. 9c). Poleward transport of tropical air occurs on isentropic surfaces via a warm conveyor belt resulting in high cloud ceiling. A small "kink" in the geopotentials which shows as a localized closed low over the study area may also account for the localized nature of the precipitation (Fig. 9cd). Small perturbations to large scale patterns are often responsible for extreme rainfall events (Woods 2006).

As the cloud band developed, negative 500 hPa vertical velocity (omega) values were observed over border of Botswana and Zimbabwe on the 12th February (Fig. 10b). Mean vertical velocity at 500 hPa from 11–13 February shows widespread upward motion supporting the development of deep convective clouds in that axis from NW-SE across the subcontinent (Fig. 10a). Negative values of omega indicate areas of rising motion (uplift) whilst negative velocity potential imply upper level divergence. Aloft, although initially unfavorable on the 11th, the velocity potential field became conducive for deep convection and rainfall as an area of upper divergence developed in the area of lifting (Fig. 10def).

At the surface, a low developed over southern Mozambique on the 11th and deepened by the 12th to about 1 008 hPa but filled to about 1 011 hPa on the day of extreme rainfall (Fig. 11abcd). A significant feature is the ridging process of a South Atlantic high pressure system which can be seen becoming more dominant on the 13th (Fig. 11c). The low over western South Africa can be seen being displaced equatorward from the 11th to the 13th. The passage of a ridging high to the south of Africa has been linked with equatorward displacement of the equatorial trough and the Inter-Tropical Convergence Zone (e.g. Suzuki, 2011). The combination of a ridging high and a surface low over southern Mozambique enhanced a NW-SE pressure gradient (Fig. 11) and moisture convergence (not shown) over the northeast of South Africa.

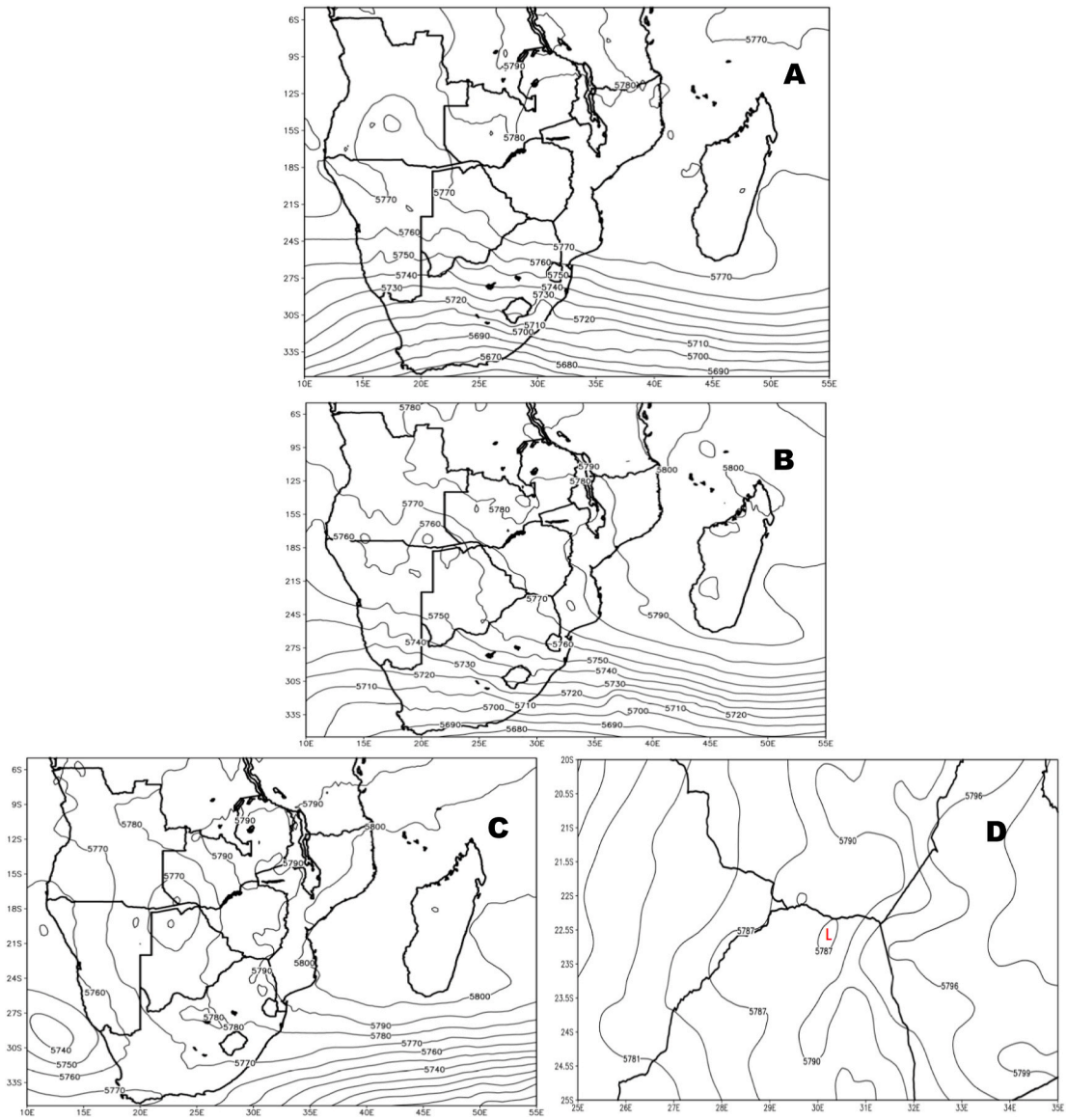

Fig. 9. Mean (18-21Z) mid-tropospheric (500 hPa) geopotential heights (meters) over southern Africa and the SWIO for (a) 11th (b) 12th and (c) February 13, 2019. A higher resolution into the study area is shown in (d) for February 13, 2019.

Ridging highs are linked to about 60% of summer rainy days over southern Africa (Ndarana et al., 2020b) while extreme rainfall observed over southern Mozambique on February 13, 2019 may be related to the presence of the surface low (Fig. 11). The geometry of the surface pressure patterns created a col field just north of the area of extreme rainfall. A col field is that area of horizontal deformation created by two lows and two highs which are juxtaposed (Cornish and Ives 2019) and may result in strong lifting or frontogenesis if temperature gradients are favorable. It is interesting that during this extreme rainfall event, the Mozambique Channel Trough (MCT; Barimalala et al., 2020) was not evident. The MCT is a cyclonic feature that develops and is dominant over the Mozambique Channel in summer. Perhaps the dominance of the surface low over the land area of Mozambique can account for this. Weak MCT activity has been linked to a positive Indian Ocean sub-tropical dipole and higher rainfall over the mainland of southern Africa (Barimalala et al., 2020).

The low-level (850 hPa) circulation was dominated by a trough over the west which developed into a deep low by the 13th (Fig. 11). The mean winds also strengthened across the region with a northeasterly component over the study area on the 11th and February 12, 2019 (Fig. 11ef) becoming easterly on the 13th (Fig. 11g). A northeasterly airflow in this region is consistent with a moisture source in the tropical Indian Ocean as identified by Rapolaki et al. (2020). At the time of extreme rainfall, wind gusts exceeding 12 m/s (~25 knots) were recorded at 10 m at Thohoyandou WO and Tshivhasie (Fig. 12) suggesting the presence of a LLJ. The wind direction at the time of the rainfall was generally southerly between southwesterly and southeasterly for the higher stations at Tshanowa and Tshivhase which aids the argument that the system propagated from the south (Thohoyandou, Fig. 12). However, winds at Thohoyandou WO veered from NE to southerly at the start of the extreme rain, becoming southwesterly and then again backing to southeasterly (Fig. 12). This wind behavior suggests the presence of a mesoscale circulation which could be analogous to a topographically trapped circulation such as happens with a coastal low over South Africa. The occurrence of coastal lows over South Africa has been detailed by Reason and Jury (1990). The presence of the mid-tropospheric closed low as shown in Fig. 9d may have compounded the interaction of low level winds with a complex topography.

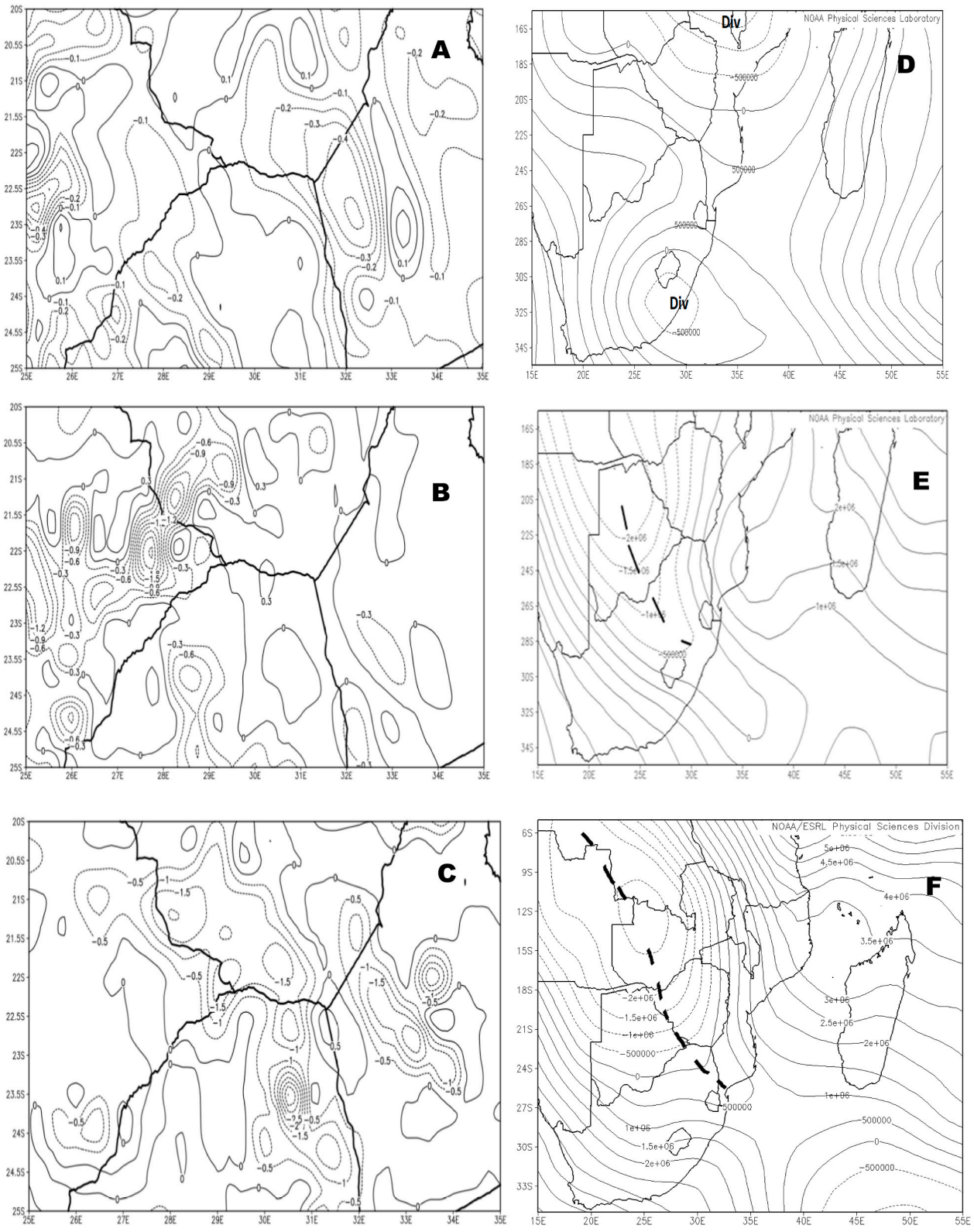

Fig. 10. Mean 18-21Z vertical velocity (omega) over the Limpopo River Valley at 500 hPa in Pas^{-1} on (a) 11th (b) 12th and (c) February 13, 2019. The corresponding velocity potential fields at $\sigma = 0.2101$ over southern Africa and the adjacent oceans are shown in panels (d) to (f).

3.5. Thermodynamic structure and orographic lifting

Whilst a large area of the Limpopo River valley in South Africa, Zimbabwe and southern Mozambique experienced heavy rainfall (>50 mm/24 h), we have shown that extreme sub-daily precipitation around Thohoyandou (200–300 mm) were localized and for a short duration. The high flooding in Thohoyandou was not only due to local rainfall but was compounded by high runoff volumes from the areas downwind but uphill from the area.

The Pretoria radiosonde profile shows the environment was

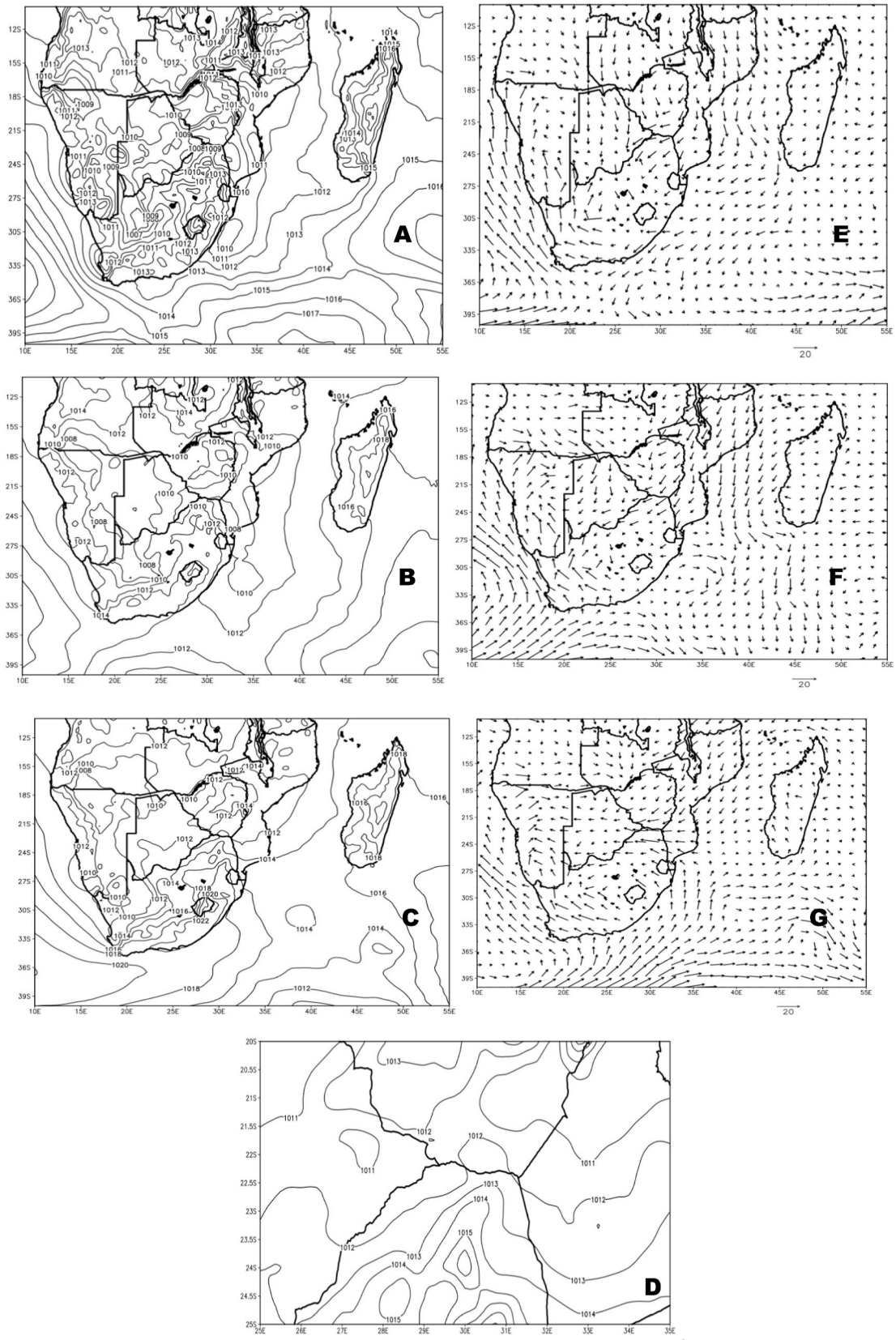

Fig. 11. Mean 18-21Z MSLP (hPa) over southern Africa and the adjacent SW Indian Ocean from (a) 11th (b) 12th (c,d) February 13, 2019. The low level (850 hPa) vector winds for the 11–13th February 2019 are shown in (e) to (g) respectively.

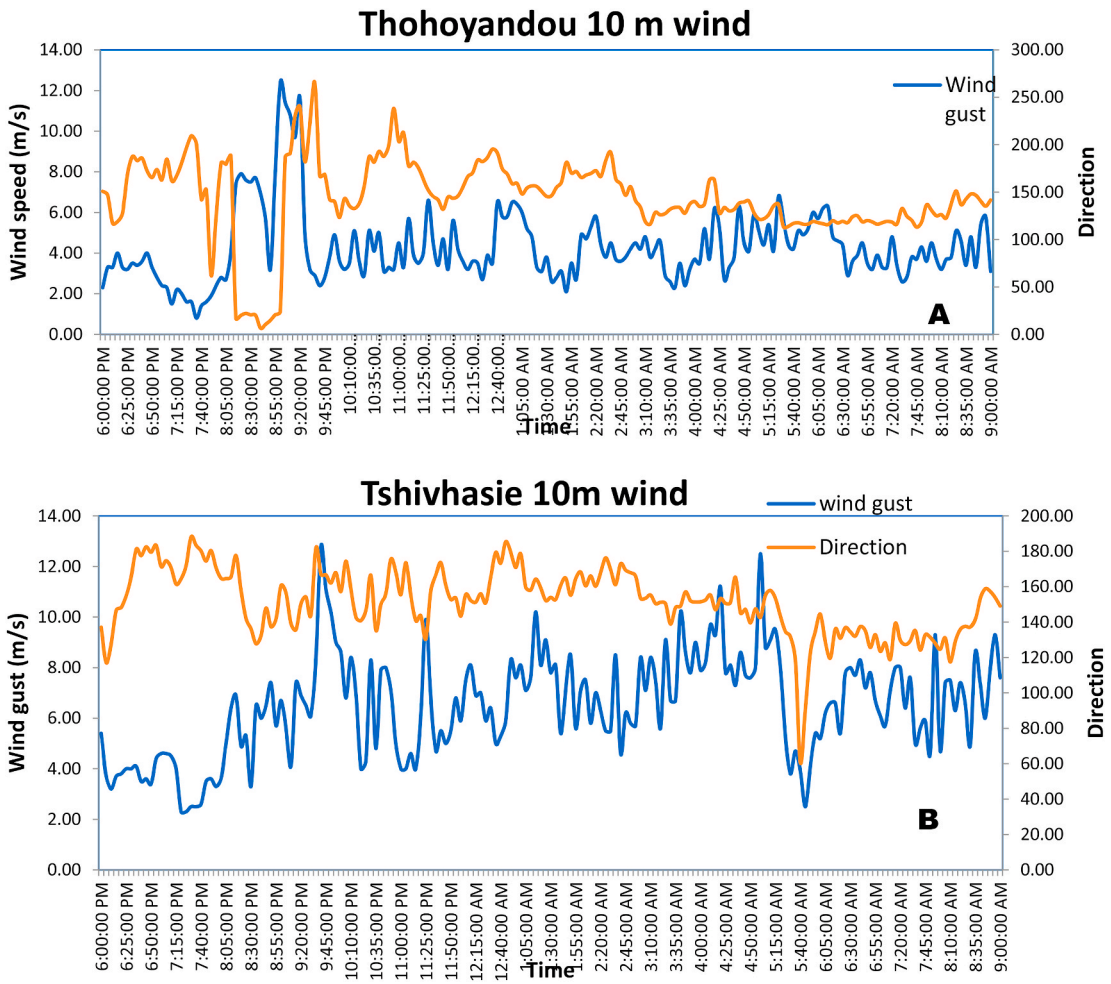

Fig. 12. Five minute wind gusts and wind direction for (a) Thohoyandou WO and (b) Tshivhasie Tea Estates from 18 h (16Z) on 13 February to 09 h (07Z) on February 14, 2019.

characterized by very moist air below 500 hPa on the 13th Feb at 12Z (Fig. 13a) becoming moist to saturated throughout the depth of the troposphere by the 14th (Fig. 13b and c) typical of tropical influence. The vertical wind profile (shown on the right hand side in barbs representing direction and strength) shows strong winds in the low levels (~800 hPa) also suggesting the presence of a LLJ from the east (Indian Ocean). Whilst the winds at Pretoria were about 25 knots on 14 February, we argue the winds were stronger in the east near the coast, due to less frictional drag (as shown in Fig. 11). We also submit that the extreme rainfall amounts shown in Table 1, Figs. 1 and 8 were enhanced by additional forcing from the complex topography of the Soutpansberg Mountain Range and the presence of a LLJ. Winds were largely northeasterly in the low levels (consistent with Fig. 11) becoming westerly aloft as expected using thermal wind arguments. Winds backing with

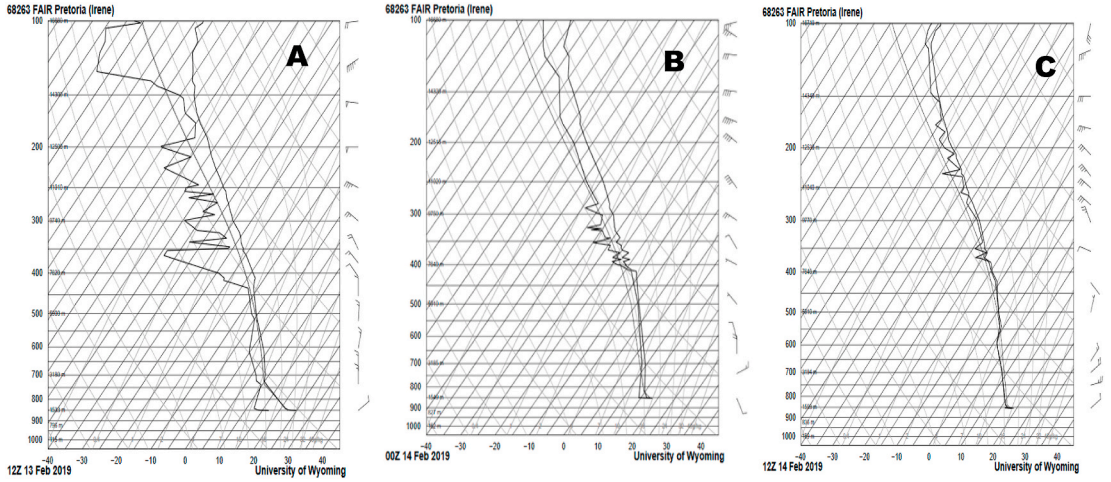

Fig. 13. Upper air sounding for Pretoria (Irene) on (a) 13 Feb 12Z and (b) 14 Feb 00Z and (c) Feb 14, 2019 at 12Z.

height in the Southern Hemisphere imply warm air advection in that layer and if accompanied by moisture advection can suggest convective (thermodynamic) instability. The surface lapse rate was conducive for convective uplift on the flood event (13th Feb 12Z) with a level of free convection of 724 hPa becoming 809 hPa by the 14th, and a high equilibrium level implying deep convection. The Convective Available Potential Energy (CAPE) was calculated at 86.78 J/kg on 14 Feb at 12Z, suggesting that dynamic activity was more dominant than convective activity in this extreme rainfall event. CAPE is a measure of the atmospheric energy available for convection and is often used by forecasters to determine the likelihood of showers and thunderstorms.

3.6. Forecasting extreme rainfall

Fig. 5 showed a rainfall band that extended from the tropics into the eastern parts of South Africa, and southern parts of Mozambique. The event was captured by UM model runs initialized with 12 February 18Z analysis. The observed hourly rainfall on the night of February 13, 2019 to the afternoon of the following day has been shown in Fig. 8a and discussed in section 3.3. Here, we compare the observed rainfall with the UM simulated hourly rainfall using data from the nearest grid point to the station (Fig. 8b). The peak in rainfall at the Thohoyandou WO and AWS is reported at 19Z, with a much higher peak at the WO of over 90 mm, while the AWS reported under 25 mm of rainfall. The Tshanowa and Tshivhase stations reported their peaks an hour later, with over 90 mm and 70 mm, respectively. Fig. 1 showed that Thohoyandou is east of Tshanowa and Tshivhase. The UM simulates the peak in rainfall at the same time at 21Z, 2 h later than the Thohoyandou peak and 1 h later than the peak in the two other stations. It is also seen that the model underestimated the amounts considerably with the model run simulating a maximum of 40 mm.

To get a better idea of the spatial distribution of rainfall, the hourly rainfall is shown in Fig. 14, ranging from 16Z–17Z to 21Z–22Z on February 13, 2019. The location of the Thohoyandou WO is indicated by a red dot. The plot shows that the UM simulated a system moving towards the west. By the end of 20Z the highest rainfall is located east of Thohoyandou WO, and this event is located over the station for the period 20Z to 21Z giving the peak as shown in Fig. 8b. The corresponding hourly radar QPE was shown in Fig. 7, and what is indicated is that the simulated rainfall structure is different to the radar QPE. The UM simulates the rainfall as part of a system extending from Mozambique, while radar QPE shows the event to be associated with a small stand-alone system. The SAWS morning forecast which is usually issued at 02.30Z included a watch of localized flooding in the western and northern parts of KwaZulu-Natal and eastern parts of Mpumalanga province. When the forecast was updated at 14Z, a watch for severe thunderstorms which could result in heavy downpours leading to localized flooding was issued for the eastern parts of Limpopo province. It may be noted that forecasts issued at SAWS do not include information on what is expected hour per hour and so the delay in rainfall would not have impacted the warnings or watches that are issued. Despite the event having been captured to some extent by the models, it found the residents of Thohoyandou not prepared. The runoff from up the slopes of the Soutpansberg had not been expected to accumulate at the Thavhani Mall (Thohoyandou) and the adjacent stadium where a professional football match was in progress and was subsequently disrupted. A recent study by Muofhe et al. (2020) evaluated the skill of the UM in forecasting COLs and also found the model to underestimate rainfall over complex topography east of South Africa.

4. Conclusions

In the middle of February 2019, an intense sub-daily rainfall event (~300 mm in less than 4 h) triggered high floods in a localized area of Thohoyandou, northeast of South Africa, consistent with a cloudburst. The extreme rainfall, high runoff and sediment yield from upslope resulted in flooding in the affected area leading to high impact, causing damage to parked cars and disrupting socio-economic activities. This paper has focused on an analysis of the meteorological structure of the event which may be considered as a compound extreme event. A compound extreme event has been defined as a combination of multiple physical processes and hazards which interact to cause high impact (Zscheischler et al., 2018). As they are rare events, they are often difficult to predict and may not have historical precedents (Milly et al., 2002). We have shown that a combination of the large-scale synoptic environment, low level winds (direction and speed), topography and propagation of heavy rain all acted to produce the high impact observed in Thohoyandou. Poor drainage systems in the urbanized location of flooding could also be a contributing factor (not shown). However, the remote forcings of the regional rainfall (SIOD, IOD and ENSO) were unfavorable for high rainfall and tropical cyclone landfalls over southern Africa during the 2018/19 rainy season and hence the motivation for this study. The entire season was mostly drier and warmer than normal over large areas of the subcontinent.

Our analyses have revealed that the synoptic circulation was dominated by a TTT in the mid-troposphere resulting in advection of tropical moisture in the form of a cloud band. This resulted in banded precipitation, extending from the tropical region (Angola) to the southeast of South Africa. During the period of extreme rain, we have shown that the low-level environmental flow was northeasterly and strengthened, whilst the mid-tropospheric geopotential field around Thohoyandou showed a localized closed low. We argue that extreme sub-daily rainfall in Thohoyandou was largely induced by mesoscale perturbations to the large scale within an already unstable environment which was intensified by a complex topography and a nearby col field. It was found in a previous study that a complex terrain can aid the generation of mesoscale circulations in South Africa or even development of mesoscale vortices (de Coning et al., 1998). Localized heavy rainfall has been linked to mesoscale perturbations to the synoptic scale on condition that the large scale environment provides favorable conditions (Lima et al., 2009). At the surface, a ridging high and a low over southern Mozambique created conditions conducive for low level convergence and uplift in the presence of a LLJ. We are also aware that a surface low is not necessarily always associated with ascending motion above them as differential development can result in isallobaric winds directed away from the center.

We have also shown that the heaviest rain fell downwind but uphill of Thohoyandou. We can conclude that the surface low created a steep pressure gradient and was important for extreme rainfall observed over Mozambique whilst interaction with mountains was more significant in Thohoyandou, the focus of this study. Mountains act to slow down the wind velocity thereby inducing low-level convergence which is associated with ascent in the mid-troposphere. The thermodynamic structure of environmental air was characterized by convectively unstable air with favorable conditions for low-level uplift and upper-air divergence.

The interaction of the surface wind and a LLJ with the steep topography compounded the event, causing enhanced lifting along the Soutpansberg Mountain Range. Weather forecasters need to look out for LLJs in regions of complex topography as they can lead to extreme rainfall events. They also need to focus more on areas of deformation in the models and the analyses, in addition to divergence and vorticity fields (Banacos 2003). This study has shown that the UM simulations delayed and underestimated the rainfall associated with this extreme event, and did not distinguish between the earlier rainfall maximum in Thohoyandou compared to the rainfall on higher ground. A high spatial resolution numerical simulation as well as local data assimilation are recommended here to investigate the role of topographic forcing due to the Soutpansberg Mountain range and the LLJ. Numerical models have the ability to isolate effects of several physical processes and determine their contribution to extreme rainfall in such a compound event. Local authorities, urban planners and civil engineers in Thohoyandou are encouraged to review drainage systems in the location of flooding to

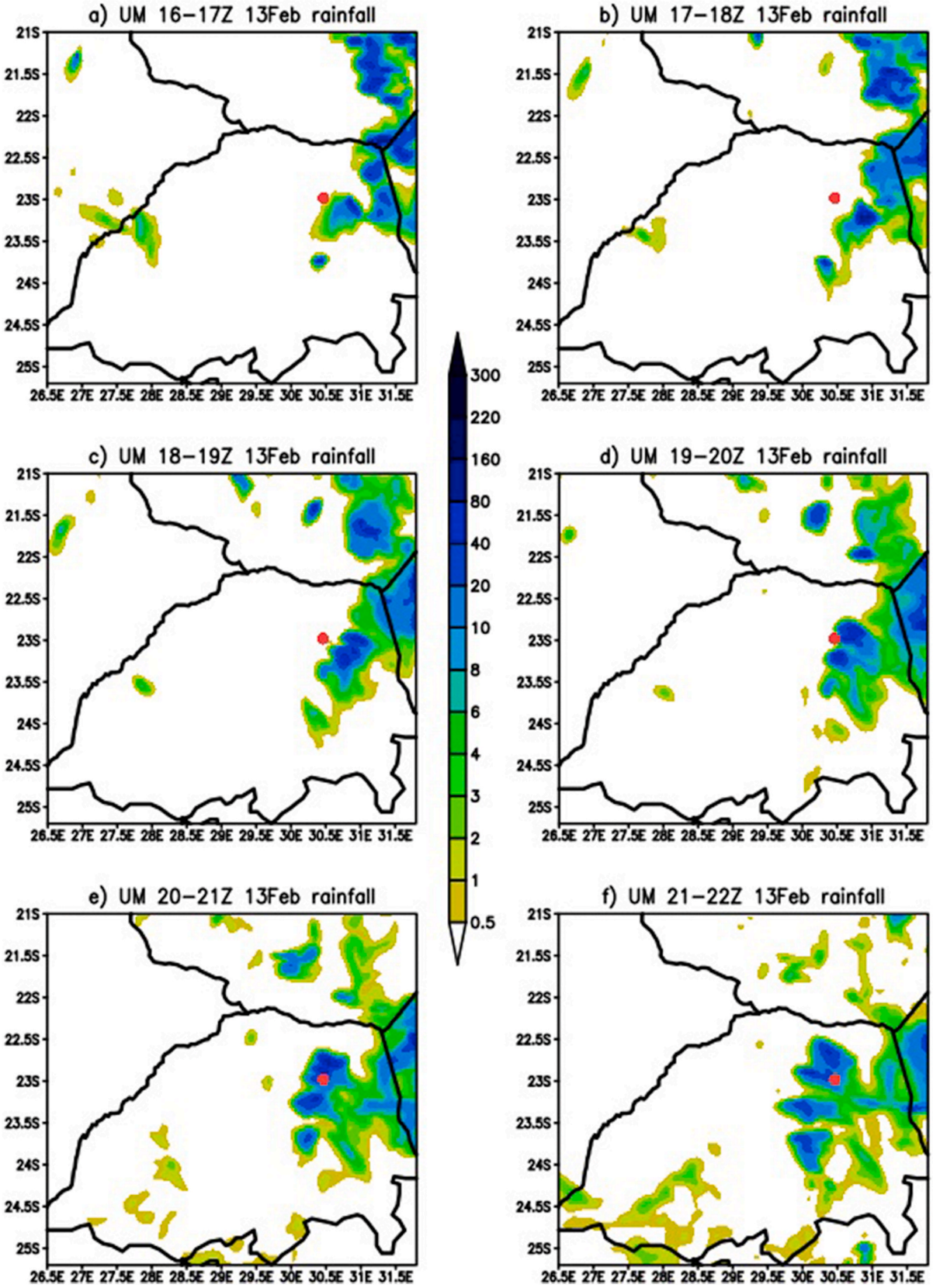

Fig. 14. UM hourly forecasts of precipitation (mm) valid for (a) 16-17Z (b) 17-18Z (c) 18-19Z (d) 19-20Z (e) 20-21Z (f) 21-22Z on February 13, 2019.

avoid a recurrence in a future event. Future developments need to be sited in areas least vulnerable to flood events.

CRediT authorship contribution statement

Hector Chikoore: Conceptualization, Resources, Investigation, Formal analysis, Writing – original draft. **Mary-Jane M. Bopape:** Software, Investigation, Data curation, Formal analysis, Writing – original draft. **Thando Ndarana:** Investigation, Resources, Methodology, Writing – original draft. **Tshimbiluni P. Muofhe:** Data curation, Formal analysis, Writing – original draft. **Morne Gijben:** Data curation, Software, Formal analysis, Writing – original draft. **Rendani B. Munyai:** Conceptualization, Methodology. **Tshilidzi C. Manyanya:** Data curation, Software, Formal analysis. **Robert Maisha:** Conceptualization, Writing – original draft.

Declaration of competing interest

The authors declare that they have no known competing financial interests or personal relationships that could have appeared to influence the work reported in this paper.

Acknowledgements

We would like to acknowledge anonymous reviewers whose comments have helped us improve the manuscript considerably. The data used in this case study was obtained from SAWS, UCSB-CHG, ECMWF, EUMETSAT, University of Wyoming and NCEP. UM simulations used here were obtained from SAWS with acknowledgements to the UK Met Office.

Appendix A. Supplementary data

Supplementary data to this article can be found online at https://doi.org/10.1016/j.wace.2021.100327.

References

Alexander, W.J.R., van Heerden, J., 1991. Determination of the Risk of Widespread Interruption of Communications by Floods. Department of Transport Research Project RDAC 90/16.

Banacos, P.C., 2003. Short-range Prediction of Banded Precipitation Associated with Deformation and Frontogenetic Forcing. Preprints, 10th Conf. On Mesoscale Processes, Portland, OR. Amer. Meteor. Soc., CD-ROM, P1.7.

Barclay, J.J., Jury, M.R., Landman, W., 1993. Climatological and structural differences between wet and dry troughs over southern Africa in the early summer. Meteorol. Atmos. Phys. 51 (1), 41–54.

Barimalala, R., Blamey, R.C., Desbiolles, F., Reason, C.J.C., 2020. Variability in the Mozambique Channel Trough and impacts on southeast African rainfall. J. Clim. 33, 749–765.

Blamey, R.C., Reason, C.J.C., 2009. Numerical simulation of a mesoscale convective system over the east coast of South Africa. Tellus 61A, 17–34.

Blamey, R.C., Reason, C.J.C., 2012. Mesoscale convective complexes over southern Africa. J. Clim. 25, 753–766.

Blamey, R.C., Kolusu, S.R., Mahlalela, P., Reason, C.J.C., 2018. The role of regional circulation features in regulating El Nino climate impacts over southern Africa: a comparison of the 2015/16 drought with previous events. Int. J. Climatol. 38 https://doi.org/10.1002/joc.5668.

Brown, A., Milton, S., Cullen, M., Golding, B., Mitchell, J., Shelley, A., 2012. Unified modelling and prediction of weather and climate: a 25-year journey. Bull. Am. Met. Soc. 93, 1865–1877.

Chikoore, H., Jury, M.R., 2010. Intraseasonal variability of satellite-derived rainfall and vegetation over southern Africa. Earth Interact. 14, 1–26.

Chikoore, H., Vermeulen, J.H., Jury, M.R., 2015. Tropical cyclones in the Mozambique channel: January-March 2012. Nat. Hazards. https://doi.org/10.1007/s11069-015-1691-0.

Chumchean, S., Sharma, A., Seed, A., 2006. An integrated approach to error correction for real-time radar-rainfall estimation. J. Atmos. Ocean. Technol. 23 (1), 67–79.

Cook, C., Reason, C.J., Hewitson, B., 2004. Wet and dry spells within particularly wet and dry summers in the South African summer rainfall region. Clim. Res. 26 (1), 17–31.

Cornish, M., Ives, E., 2019. Reeds Marine Meteorology, *fourth ed.* Bloomsbury Publishing, p. 256.

Crimp, S.J., Mason, S.J., 1998. The extreme precipitation event of 11–16 February 1996 over South Africa. Meteorol. Atmos. Phys. 70, 29–42.

Crimp, S.J., Lutjeharms, J.R.E., Mason, S.J., 1998. Sensitivity of a tropical-temperate trough to sea-surface temperature anomalies in the Agulhas retroflection region. WaterSA 24, 93–100.

Davies, T., Cullen, M.J.P., Malcolm, A.J., Mawson, A.S.M.H., White, A.A., Wood, N., 2005. A new dynamical core for the Met Office's global and regional modelling of the atmosphere. Quart. J. Roy Meteor. Soc. 131, 1759–1782.

D'Abreton, P.C., Lindesay, J.A., 1993. Water vapour transport over southern Africa during wet and dry early and late summer months. Int. J. Climatol. 13, 151–170.

D'Abreton, P.C., Tyson, P.D., 1995. Divergent and non-divergent water vapour transport over southern Africa during wet and dry conditions. Meteorol. Atmos. Phys. 55, 47–59.

de Coning, E., Forbes, G.S., Poolman, E., 1998. Heavy precipitation and flooding on 12-14 February 1996 over the summer rainfall regions of South Africa: synoptic and isentropic analyses. Natl. Weather Digest 22, 25–36.

de Coning, E., Gijben, M., Maseko, B., van Hemert, L., 2015. Using satellite data to identify and track intense thunderstorms in South and Southern Africa. South Afr. J. Sci. 111 https://doi.org/10.17159/sajs.2015/20140402.

Dyson, L.L., 2009. Heavy daily-rainfall characteristics over the Gauteng Province. WaterSA 35, 627–638.

Dyson, L.L., van Heerden, J., 2001. The heavy rainfall and floods over the northeastern interior of South Africa during February 2000. South Afr. J. Sci. 97, 80–86.

Dyson, L.L., van Heerden, J., 2002. A model for the identification of tropical weather systems over South Africa. WaterSA 28, 249–258.

Dyson, L.L., van Heerden, J., Sumner, P., 2015. A baseline climatology of sounding-derived parameters associated with heavy rainfall over Gauteng, South Africa. Int. J. Climatol. 35, 114–127.

Engelbrecht, C.J., Engelbrecht, F.A., Dyson, L.L., 2013. High-resolution model-projected changes in mid-tropospheric closed lows and extreme rainfall events over southern Africa. Int. J. Climatol. 33, 173–187.

Fauchereau, N., Pohl, B., Reason, C.J.C., Rouault, M., Richard, Y., 2009. Recurrent daily OLR patterns in the Southern Africa/Southwest Indian Ocean region, implications for South African rainfall and teleconnections. Clim. Dynam. 32, 575–591.

Favre, A., Hewitson, B., Lennard, C., Cerexo-Mota, R., Tadross, M., 2013. Cut-off lows in the South African region and their contribution to precipitation. Clim. Dynam. 41, 2331–2351.

Funk, C., Peterson, P., Landsfeld, M., Co-Authors, 2015. The climate hazards infrared precipitation with stations – a new environmental record for monitoring extremes. Sci. Data 2. https://doi.org/10.1038/sdata.2015.66.

Gordon, N., Shaykewich, J., 2000. Guidelines on Performance Assessment of Public Weather Services, World Meteorological Organisation. WMO/TD No.1023, p. 32.

Harangazo, S., Harrison, M.S.J., 1983. On the use of synoptic data indicating the presence of cloud bands over southern Africa. South Afr. J. Sci. 79, 413.

Harrison, M.S.J., 1984. A generalized classification of South African summer rain-bearing synoptic systems. J. Climatol. 4, 547–560.

Hart, N., Reason, C., Fauchereau, N., 2010. Tropical-extratropical interactions over southern Africa: three cases of heavy summer season rainfall. Mon. Weather Rev. 138, 2608–2623.

Hart, N., Reason, C., Fauchereau, N., 2013. Cloud bands over southern Africa: seasonality, contribution to rainfall variability and modulation by the MJO. Clim. Dynam. 41 https://doi.org/10.1007/s00382-012-1589-4.

Hart, N.C.G., Washington, R., Reason, C.J.C., 2018. On the likelihood of tropical-extratropical cloud bands in the South Indian Convergence Zone during ENSO events. J. Clim. 31, 2797–2817.

Hersbach, H., Bell, B., Berrisford, P., co-authors, 2020. The ERA5 global reanalysis. Quart. J. Roy. Met. Soc. https://doi.org/10.1002/qj.3803.

Jury, M.R., 2010. Flood-producing cloud bands over the Kalahari Desert. Theor. Appl. Climatol. 102, 367–378.

Kalnay, E., Kanamitsu, M., Kistler, R., co-authors, 1996. The NCEP/NCAR 40 year reanalysis project. Bull. Am. Met. Soc. 77, 437–471.

Kendon, E.J., Stratton, R.A., Tucker, S., co-authors, 2019. Enhanced future changes in wet and dry extremes over Africa at convection-permitting scale. Nat. Commun. 10 https://doi.org/10.1038/s41467-019-09776-9.

Kolstad, E.W., 2020. Prediction and precursors of Idai and 38 other tropical cyclones and storms in the Mozambique Channel. Quart. J. Roy. Met. Soc. https://doi.org/10.1002/qj.3903.

Kruger, A.C., Nxumalo, M.P., 2017. Historical rainfall trends in South Africa: 1921-2015. WaterSA 43. https://doi.org/10.4314/wsa.v43i2.12.

Kuo, H.L., Seitter, K.L., 1985. Instability of shearing geostropic currents in neutral and partly unstable atmospheres. J. Atmos. Sci. 42, 331–345.

Levey, K.M., Jury, M.R., 1996. Composite intraseasonal oscillations of convection over southern Africa. J. Clim. 9, 1910–1920.

Lima, K.C., Satyamurty, P., Fernandez, J.P.R., 2009. Large-scale atmospheric conditions associated with heavy rainfall episodes in southeast Brazil. Theor. Appl. Climatol. 101, 121–*135*.

Lindesay, J., 1998. In: Hobbs, J.E., Lindesay, J.A., HA, Bridgman (Eds.), Present Climate of Southern Africa. I: Climates of the Southern Continents. Past, Present and Future. John Wiley and Sons, Chichester, p. 297.

Lindesay, J., Jury, M.R., 1991. Atmospheric circulation controls and characteristics of a flood event in central South Africa. Int. J. Climatol. 11, 609–627.

Liu, H., He, M., Wang, B., Zhang, Q., 2014. Advances in low-level jet research and future prospects. J. Meteorol. Res. 28, 58–75.

MacKellar, N., New, M., Jack, C., 2014. Observed and modelled trends of temperature and rainfall for South Africa: 1960-2010. South Afr. J. Sci. 110 https://doi.org/10.1590/sajs.2014/20130353.

Maisha, T.R., 2014. The Influence of Topography and Model Grid Resolution on Extreme Weather Forecasts over South Africa. *MSc dissertation, University of Pretoria*.
Manatsa, D., Matarira, C.H., 2009. Changing dependence of Zimbabwean rainfall variability on ENSO and the Indian Ocean dipole/zonal mode. Theor. Appl. Climatol. https://doi.org/10.1007/s00704-007-0315-3.
Marshall, J.S., Palmer, W.K.M., 1948. The distribution of raindrops with size. J. Meteorol. 5, 165–166.
Mason, S.J., Jury, M.R., 1997. Climate variability and change over southern Africa: a reflection on underlying processes. Prog. Phys. Geogr. 21, 23–50.
Mawren, D., Hermes, J., Reason, C.J.C., 2020. Exceptional tropical cyclone Kenneth in the far northern Mozambique Channel and ocean eddy influences. Geophys. Res. Lett. 47, e2020GL088715.
Milly, P.C.D., Wetherhald, R.T., Dunne, K.A., Delworth, T.L., 2002. Increasing risk of great floods in a changing climate. Nature 415, 514–517.
Muller, A., Reason, C.J.C., Fauchereau, N., 2008. Extreme rainfall in the Namib Desert during late summer 2006 and influences of regional ocean variability. Int. J. Climatol. 28, 1061–1071.
Muofhe, T.P., Chikoore, H., Bopape, M.M., Nethengwe, N.S., Ndarana, T., Rambuwani, G.T., 2020. Forecasting intense cut-off lows over South Africa using the 4.4 km Unified Model. Climate 8, 129. https://doi.org/10.3390/cli8110129.
Ndarana, T., Waugh, D.W., 2010. The link between cut-off lows and Rossby wave breaking in the Southern Hemisphere. Q. J. R. Meteorol. Soc. 136 https://doi.org/10.1002/qj.627.
Ndarana, T., Rammopo, T.S., Chikoore, H., Barnes, M.A., Bopape, M., 2020a. A quasi-geostrophic diagnosis of the zonal flow associated with cut-off lows over South Africa and surrounding oceans. Clim. Dynam. https://doi.org/10.1007/s00382-020-05401-4.
Ndarana, T., Mpati, S., Bopape, M., Engelbrecht, F., Chikoore, H., 2020b. The flow and moisture fluxes associated with ridging South Atlantic Ocean anticyclones during the subtropical southern African summer. Int. J. Climatol. https://doi.org/10.1002/joc.6745.
New, M., Hewitson, B., Stephenson, D.B., Co-Authors, 2006. Evidence of trends in daily climate extremes over southern and West Africa. J. Geophys. Res. 111, D14102 https://doi.org/10.1029/2005JD006289.
Rapolaki, R.S., Blamey, R.C., Hermes, J.C., Reason, C.J.C., 2019. A classification of synoptic weather patterns linked to extreme rainfall over the Limpopo River Basin in southern Africa. Clim. Dynam. 53, 2265–2279.
Rapolaki, R.S., Blamey, R.C., Hermes, J.C., Reason, C.J.C., 2020. Moisture sources associated with heavy rainfall over the Limpopo River Basin, southern Africa. Clim. Dynam. https://doi.org/10.1007/s00382-020-05336-w.
Rapolaki, R.S., Reason, C.J.C., 2018. Tropical storm Chedza and associated floods over south-eastern Africa. Nat. Hazards 93, 189–217.
Rasmussen, E.N., Do Blanchard, 1998. A baseline climatology of sounding-derived supercell and tornado forecast parameters. Weather Forecast. 13, 1148–1164.
Ratnam, J.V., Behera, S.K., Masumoto, Y., Yamagata, T., 2014. Remote effects of El Niño and Modoki events on the austral summer precipitation of southern Africa. J. Clim. 27, 3802–3815.
Reason, C.J.C., Jury, M.R., 1990. On the generation and propagation of the southern African coastal low. Q. J. R. Meteorol. Soc. 116, 1133–1151.
Reason, C.J.C., Kiebel, A., 2004. Tropical cyclone Eline and its unusual penetration and impacts over the southern African mainland. Weather Forecast. 19, 789–805.
Reason, C.J.C., 2007. Tropical cyclone Dera, the unusual 2000/01 tropical cyclone season in the southwest Indian Ocean and associated rainfall anomalies over southern Africa. Meteorol. Atmos. Phys. 97, 181–188.
Reynolds, R.W., 1993. Impact of Mount Pinatubo aerosols on satellite-derived sea surface temperatures. J. Clim. 6, 768–774.
Roy, S.S., Rouault, M., 2013. Spatial patterns of seasonal scale trends in extreme hourly precipitation in South Africa. Appl. Geogr. 39, 151–157.
Saji, H., Goswami, B.N., Vinayachandran, P., Yamagata, T., 1999. A dipole mode in the tropical Indian Ocean. Nature 401, 360–363.
Simpson, L., Dyson, L.L., 2018. Severe weather over the Highveld of South Africa during November 2016. WaterSA 44, 75–85.
Singleton, A.T., Reason, C.J.C., 2006. Numerical simulations of a severe rainfall event over the Eastern Cape coast of South Africa: sensitivity to sea surface temperature and topography. Tellus Dyn. Meteorol. Oceanogr. 58, 335–367.
Singleton, A.T., Reason, C.J.C., 2007a. A numerical model study of an intense cut-off low pressure system over South Africa. Mon. Weather Rev. 135, 1128–1150.
Singleton, A.T., Reason, C.J.C., 2007b. Variability in the characteristics of cut-off low pressure systems over subtropical southern Africa. Int. J. Climatol. 27, 295–310.
Steiner, M., Smith, J.A., Burges, S.J., Alonso, C.V., Darden, R.W., 1999. Effect of bias adjustment and rain gauge data quality control on radar rainfall estimation. Water Resour. Res. 35 (8), 2487–2503.
Stensrud, D.J., 1996. The importance of low-level jets to climate: a review. J. Clim. 9, 1698–17-11.
Suzuki, T., 2011. Seasonal variation of the ITCZ and its characteristics over central Africa. Theor. Appl. Climatol. 103, 39–60.
Taljaard, J.J., 1985. In: Cut-off Lows in the South African Region. S. Afr.Weather Serv. Tech. Pap. 14, S. Afr. Weath. Serv. Private Bag X097, Pretoria.
Todd, M.C., Washington, R., 1999. Circulation anomalies associated with tropical-temperate troughs over southern Africa. Clim. Dynam. 15, 937–951.
Trenberth, K.E., 1999. Atmospheric moisture recylcling: role of advection and local evaporation. J. Clim. 12, 1368–1381.
Trenberth, K.E., Dai, A., Rasmussne, R.M., Parsons, D.B., 2003. The changing character of precipitation. Bull. Am. Met. Soc. 84, 1205–1218.
Woods, A., 2006. Medium Range Weather Prediction: the European Approach – the Story of the European Center for Medium-Range Weather Forecasts. Springer, New York NY, p. 270.
Zhao, Y., 2012. Numerical investigation of a localized extremely heavy rainfall event in complex topographic area during midsummer. Atmos. Res. 113, 22–39.
Zscheischler, J., Westra, S., van den Hurk, B.J.J.M., Co-authors, 2018. Future climate risk from compound events. Nat. Clim. Change 8, 469–477.